Dynamic Operating Envelopes-enabled Demand Response in Low-voltage Residential Networks

Gayan Lankeshwara* and Rahul Sharma†
School of Information Technology and Electrical Engineering,
The University of Queensland,
Brisbane, QLD 4072, Australia.
Email: *g.lankeshwara@uqconnect.edu.au, †rahul.sharma@uq.edu.au

***Abstract*—This paper presents a real-time, coordinated approach for residential demand response (DR) participation in electricity markets under the dynamic operating envelopes (DOEs) framework. In the first stage, the distribution network service provider (DNSP) utilises a *convex hull* method to construct DOEs at each customer point-of-connection (PoC). In the second stage, the demand response aggregator (DRA) employs a hierarchical control framework for tracking a load set-point signal commanded by the market operator while individual households minimise their electricity costs. In this regard, the real-time control operation takes account of DOEs assigned by the DNSP. The simulation results validated on a real Australian network with realistic data suggest that the DRA is able to achieve precise tracking of the load set-point signal while honouring network statutory limits and also managing comfort for end-users. Furthermore, the approach preserves end-user privacy and is scalable.**

***Index Terms*—Demand response, dynamic operating envelopes, low-voltage distribution networks, import/export limits, network statutory limits, air-conditioners**

I. Introduction

The rapid penetration of behind-the-meter distributed energy resources (DERs) in low-voltage (LV) networks and their participation in demand response (DR) and other electricity market services have created complex technical challenges for distribution network service providers (DNSPs) to manage network integrity. One strategy to overcome these challenges is to impose fixed import/export limits and curtail excess consumption/generation beyond the pre-defined limit. For instance, in Queensland, a 5 kW export limit is introduced for small customer connections [1]. However, static limits are based on worst-case loading and generation scenarios and often underutilise the available capacity of DERs.

Dyanmic operating envelopes (DOEs) is an insightful approach that takes account of the dynamic behaviour of household load and generation in determining import/export limits. As defined in [2], "Dynamic operating envelopes vary import and export limits over time and location based on the available capacity of the local network or power system as a whole." Based on this definition, DOEs can be implemented at either DER-level or at the point of connection (PoC) of an end-user.

978-1-6654-6738-4/22/$31.00 ©2022 IEEE

Considering the state-of-the-art literature, strategies for implementing DOEs for households can be discussed under two groups: 1) optimal power flow (OPF)-based approaches; 2) network sensitivity-based approaches. In OPF-based approaches, an optimisation problem is formulated to maximise the utility and/or social welfare of the DNSP while taking account of network statutory limits, DER operational limits. The solution gives optimal power set-points for customer connections and individual DERs such that network technical limits are honoured. For instance, the authors in [3] have introduced a centralised control scheme based on AC-OPF such that end-user export limits are maximised. Along with that, the DNSP accounts for network statutory limits. In [4], a two-level control strategy based on OPF is proposed to assign active power set-points for household battery storage. In this approach, DOEs are assigned only if the end-user intended operation compromises voltage limits of the network. However, end-users are required to send information on their consumption and generation periodically to the DNSP. This will lead to data privacy issues. To alleviate privacy issues, the authors in [5] have proposed a hierarchical control scheme based on the alternating direction method of multipliers (ADMM) where network-secure envelopes are determined for consumer-owned rooftop photovoltaic (PV) and battery storage to provide services in electricity markets. Furthermore, this approach also accommodates end-user reactive power through a Q-P controller.

In network sensitivity-based approaches, the sensitivity of voltage and current with respect to active and reactive power are determined for a certain operating state of the network via perturb-and-disturb method, numerical calculations, and regression. Thereafter, sensitivity factors are used to determine nodal injections of active and reactive power such that network constraints are honoured. For example, the authors in [6] have proposed a network-aware approach for the participation of DR in day-ahead and real-time markets. In this method, the DNSP calculates network sensitivity factors via regression and shares with the demand response aggregator (DRA) for its market participation. In [7], a network-aware method based on distributed model predictive control (MPC) and ADMM is utilised for DERs to track a day-ahead dispatch plan and for the operation in real-time. Furthermore, an analytical approach is occupied to determine network sensitivities.

To this end, most of the existing studies focus on developing a DOE framework to assign export limits to cater for the strong uptake of PV and battery storage in residential networks. In this regard, the contribution of residential DR is often overlooked in the formulation. Hence, household import limits are paid much less attention in the current practice compared to dynamic export limits [2]. However, it should be noted that exporting rooftop PV generation to the grid along with participation in DR services could have an adverse impact on the network. Despite the consideration of DR in [6], the overall centralised approach requires end-users to share sensitive information with the DNSP and the DRA. This gives rise to end-user data privacy concerns. Hence, developing a privacy-preserving control framework is crucial for a real-world implementation.

The main contributions of this work can be summarised as:

- Developing a two-stage, coordinated, real-time control scheme for dynamic operating envelopes-enabled demand response in low-voltage networks.
- Preserving end-user privacy via a hierarchical implementation based on the ADMM form of the resource-sharing problem.
- Dynamic operating envelopes take account of active/reactive and import/export power limits.

The rest of the paper is organised as follows. Section II outlines the proposed methodology. The simulation studies are discussed in section III and concluding remarks are presented in section IV.

II. Proposed Methodology

In this work, a two-stage coordinated approach is proposed for the DOE-enabled real-time demand management in residential LV networks. A summarised block diagram of the proposed approach is given in Fig. 1. The overall approach can be described under two stages. In stage I, the DNSP determines household DOEs based on power injection limits at PoC and sends to the DRA. In stage II, the DRA utilises the dynamic operating envelopes calculated in the previous stage to provide DR services in electricity markets while concurrently satisfying network statutory limits.

Let $\mathcal{H} := \{1, 2, \ldots, H\}$ be the set of households indexed by h and $\mathcal{T} := \{t_0, t_1, \ldots, t_0 + T\}$ be the set of time periods indexed by t. Since end-users with embedded generation can only adopt dynamic connections in Queensland, the following disjoint sets of residential customers are defined: 1) *DOE customers* — end-users with rooftop PV and adopt DOEs ($\mathcal{H}^{++} \subseteq \mathcal{H}$); 2) *non-DOE customers*— end-users with rooftop PV and do not adopt DOEs ($\mathcal{H}^{+} \subseteq \mathcal{H}$); 3) *passive customers*—end-users without rooftop PV ($\mathcal{H}^{-} \subseteq \mathcal{H}$). Furthermore, *DOE customers* will only participate in DR events. The steps involved in the overall process of DOE-enabled DR are discussed in detail in the following sections.

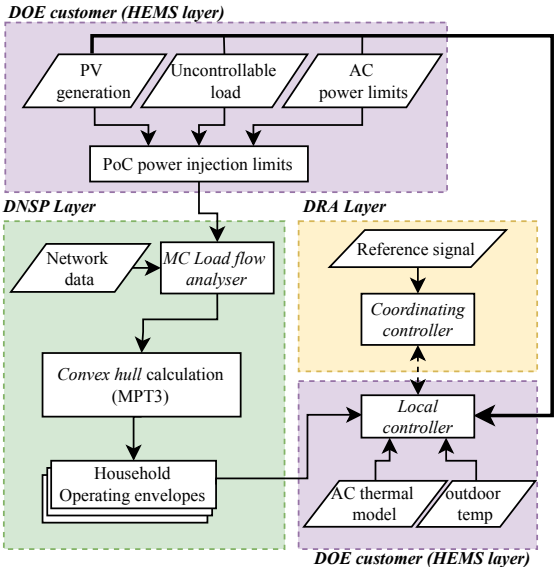

Fig. 1. A summarised block diagram of the proposed approach

A. Stage I: DNSP determining household operating envelopes

The process of DNSP estimating household operating envelopes consists of two steps: 1) households calculating power injection limits at the PoC; 2) DNSP constructing household operating envelopes based on a combination of Monte Carlo (MC) load flows studies and *convex hull* approximation.

1) Households determining power injection limits

In the first stage of the two-stage approach, the DNSP is required to determine household DOEs in real-time. Considering the inverter-type air-conditioner—thermal model described by [8]—to be the controllable DER present in each *DOE customer*, the active and reactive power injection at the point-of-connection (PoC) of household $h \in \mathcal{H}^{++}$ at time $t \in \mathcal{T}$ can be expressed as:

$$P^{h}_{\mathrm{inj},t} = \tilde{P}^{h}_{\mathrm{PV},t} - P^{h}_{\mathrm{AC},t} - \tilde{P}^{h}_{\mathrm{UL},t} \tag{1}$$

$$Q^{h}_{\mathrm{inj},t} = \tilde{Q}^{h}_{\mathrm{PV},t} - Q^{h}_{\mathrm{AC},t} - \tilde{Q}^{h}_{\mathrm{UL},t} \tag{2}$$

where $P^{h}_{\mathrm{inj},t}$ and $Q^{h}_{\mathrm{inj},t}$ corresponds to active and reactive power injection, $\tilde{P}^{h}_{\mathrm{PV},t}$ and $\tilde{Q}^{h}_{\mathrm{PV},t}$ corresponds to available active and reactive power generation of rooftop PV, $P^{h}_{\mathrm{AC},t}$, $Q^{h}_{\mathrm{AC},t}$ corresponds to active and reactive power consumption of the air-conditioner, $\tilde{P}^{h}_{\mathrm{UL},t}$ and $\tilde{Q}^{h}_{\mathrm{UL},t}$ corresponds to active and reactive power consumption of uncontrollable loads of household h at time t. In this regard, $P^{h}_{\mathrm{inj},t} > 0$ represents exporting power to the grid whereas $P^{h}_{\mathrm{inj},t} < 0$ represents importing power from the grid at time t.

For the controllable air-conditioning load, active power is bounded by,

$$0 \leq P^{h}_{\mathrm{AC},t} \leq \overline{P}^{h}_{\mathrm{AC}} \tag{3}$$

where $\overline{P}^{h}_{\mathrm{AC}}$ is the rated power of the inverter-type air-conditioner at house $h \in \mathcal{H}^{++}$. Furthermore, it is assumed that the active power factor correction method [9] is employed for the operation of the air-conditioner. Following this, the

relationship between $P^h_{\mathrm{AC},t}$ and $Q^h_{\mathrm{AC},t}$ at time t can be expressed as:

$$Q^h_{\mathrm{AC},t} = P^h_{\mathrm{AC},t} \cdot \tan\left(\cos^{-1}\left(\varphi^h_{\mathrm{AC}}\right)\right) \tag{4}$$

where φ^h_{AC} is the constant power factor (lagging) for the inverter-type air-conditioner at household $h \in \mathcal{H}^{++}$.

Since rooftop PV generation is considered to be uncontrollable, fixed power factor operation in line with *AS/NZS 4777.2* standards [10] is assumed. Hence, $\tilde{Q}_{\mathrm{PV},t}$ of rooftop PV in house $h \in \mathcal{H}^{++}$ can be obtained as:

$$\tilde{Q}^h_{\mathrm{PV},t} = \tilde{P}^h_{\mathrm{PV},t} \cdot \tan\left(\cos^{-1}\left(\varphi^h_{\mathrm{PV}}\right)\right) \tag{5}$$

where φ^h_{PV} corresponds to the power factor of the rooftop PV inverter at house $h \in \mathcal{H}^{++}$.

Similarly, for uncontrollable load, fixed power factor operation is assumed. Hence, the following relationship exists.

$$\tilde{Q}^h_{\mathrm{UL},t} = \tilde{P}^h_{\mathrm{UL},t} \cdot \tan\left(\cos^{-1}\left(\varphi^h_{\mathrm{UL}}\right)\right) \tag{6}$$

where φ^h_{UL} corresponds to the power factor of the uncontrollable load at house $h \in \mathcal{H}^{++}$.

Following this, the minimum and maximum limits of active and reactive power injection at the PoC of household $h \in \mathcal{H}^{++}$ at time t can be algebraically calculated as:

$$\underline{P}^h_{\mathrm{inj},t} = \min\left(P^h_{\mathrm{inj},t}\right) \quad \text{s.t. (1)} - \text{(6)} \tag{7}$$

$$\overline{P}^h_{\mathrm{inj},t} = \max\left(P^h_{\mathrm{inj},t}\right) \quad \text{s.t. (1)} - \text{(6)} \tag{8}$$

$$\underline{Q}^h_{\mathrm{inj},t} = \min\left(Q^h_{\mathrm{inj},t}\right) \quad \text{s.t. (1)} - \text{(6)} \tag{9}$$

$$\overline{Q}^h_{\mathrm{inj},t} = \max\left(Q^h_{\mathrm{inj},t}\right) \quad \text{s.t. (1)} - \text{(6)} \tag{10}$$

For instance, $\underline{P}^h_{\mathrm{inj},t}$ in (7) can be calculated by setting $P^h_{\mathrm{AC},t}$ at its maximum value which is $\overline{P}^h_{\mathrm{AC}}$ according to (3). This is because the air-conditioner is the controllable load in DR and the active power injection at the PoC varies according to the value of $P^h_{\mathrm{inj},t}$. Following a similar approach, $\overline{P}^h_{\mathrm{inj},t}$ in (8) can be calculated by setting $P^h_{\mathrm{AC},t}$ at its minimum value which is zero.

For *non-DOE customers*, i.e., $h \in \mathcal{H}^{+}$, since the air-conditioning load is uncontrollable and cannot participate in DR, (1) and (2) simplifies to:

$$P^h_{\mathrm{inj},t} = \tilde{P}^h_{\mathrm{PV},t} - \tilde{P}^h_{\mathrm{UL},t} \tag{11}$$

$$Q^h_{\mathrm{inj},t} = \tilde{Q}^h_{\mathrm{PV},t} - \tilde{Q}^h_{\mathrm{UL},t} \tag{12}$$

Since rooftop PV generation is also uncontrollable, active and reactive power limits at the PoC can be obtained as: $P^h_{\mathrm{inj},t} = \underline{P}^h_{\mathrm{inj},t} = \overline{P}^h_{\mathrm{inj},t}$ and $Q^h_{\mathrm{inj},t} = \underline{Q}^h_{\mathrm{inj},t} = \overline{Q}^h_{\mathrm{inj},t}$ subject to (5) and (6) for $h \in \mathcal{H}^{+}$.

For *passive customers*, i.e., $h \in \mathcal{H}^{-}$, (1) and (2) further simplifies to:

$$P^h_{\mathrm{inj},t} = -\tilde{P}^h_{\mathrm{UL},t} \tag{13}$$

$$Q^h_{\mathrm{inj},t} = -\tilde{Q}^h_{\mathrm{UL},t} \tag{14}$$

Similar to *non-DOE customers*, active and reactive power injection limits for *passive customers* can be obtained as: $P^h_{\mathrm{inj},t} = \underline{P}^h_{\mathrm{inj},t} = \overline{P}^h_{\mathrm{inj},t}$ and $Q^h_{\mathrm{inj},t} = \underline{Q}^h_{\mathrm{inj},t} = \overline{Q}^h_{\mathrm{inj},t}$ subject to (6) for $h \in \mathcal{H}^{-}$.

Once $\left[\underline{P}^h_{\mathrm{inj},t}, \overline{P}^h_{\mathrm{inj},t}, \underline{Q}^h_{\mathrm{inj},t}, \overline{Q}^h_{\mathrm{inj},t}\right]$ is calculated locally [1] for all $h \in \mathcal{H}$ for the next time step, the information is passed to the DNSP.

2) Constructing dynamic operating envelopes for households

With information from power injection limits at the PoC for all $h \in \mathcal{H}$ at a particular time step, the DNSP utilises a *bounding-box approximation* method to determine the region of operation in the P-Q plane for each *DOE-customer*. Considering household $h \in \mathcal{H}^{++}$ at time $t \in \mathcal{T}$, the bounding box $\mathfrak{B}^h_t$ which captures the overall region of operation is given by:

$$\mathfrak{B}^h_t := \left\{ \left(P^h_{\mathrm{inj},t}, Q^h_{\mathrm{inj},t}\right) \;\middle|\; \begin{array}{l} \underline{P}^h_{\mathrm{inj},t} \le P^h_{\mathrm{inj},t} \le \overline{P}^h_{\mathrm{inj},t} \\ \underline{Q}^h_{\mathrm{inj},t} \le Q^h_{\mathrm{inj},t} \le \overline{Q}^h_{\mathrm{inj},t} \end{array} \right\} \tag{15}$$

The bounding box in (15) represents the capability curve at the PoC for each *DOE-customer* at time $t \in \mathcal{T}$. However, there is no guarantee that all combinations of $\left(P^h_{\mathrm{inj},t}, Q^h_{\mathrm{inj},t}\right) \in \mathfrak{B}^h_t$ for $h \in \mathcal{H}^{++}$ would honour voltage statutory limits of the network. Hence, the DNSP further utilises MC simulation studies to determine feasible pairs of $\left(P^h_{\mathrm{inj},t}, Q^h_{\mathrm{inj},t}\right) \in \mathfrak{B}^h_t$ such that resulting three-phase unbalanced load flows would not breach voltage limits at any node $i \in \mathcal{N}$ of the network. To this end, it is assumed that the DNSP has full information on network configuration and parameters to perform load flow studies.

Let Ω be the set of MC scenarios indexed by ω at time $t \in \mathcal{T}$ and $\left(P^{h,\omega}_{\mathrm{inj},t}, Q^{h,\omega}_{\mathrm{inj},t}\right)$ be the pair of active and reactive power injection at the PoC of house $h \in \mathcal{H}^{++}$ under scenario ω at time t. For house $h \in \mathcal{H}^{++}$, $\left(P^{h,\omega}_{\mathrm{inj},t}, Q^{h,\omega}_{\mathrm{inj},t}\right)$ are chosen from a uniform distribution such that $P^{h,\omega}_{\mathrm{inj},t} \in \mathcal{U}(\underline{P}^h_{\mathrm{inj},t}, \overline{P}^h_{\mathrm{inj},t})$ and $Q^{h,\omega}_{\mathrm{inj},t} \in \mathcal{U}(\underline{Q}^h_{\mathrm{inj},t}, \overline{Q}^h_{\mathrm{inj}})$. On the other hand, since $\left(P^h_{\mathrm{inj},t}, Q^h_{\mathrm{inj},t}\right)$ are fixed for $h \in \mathcal{H}^{+} \cup \mathcal{H}^{-}$, the bounding-box in (15) simplifies to a single point in the P-Q plane. Hence, $\left(P^{h,\omega}_{\mathrm{inj},t}, Q^{h,\omega}_{\mathrm{inj},t}\right)$ is considered to be fixed for all $\omega \in \Omega$. Thereafter, a three-phase unbalanced load flow [11] is performed to determine whether $\left(P^{h,\omega}_{\mathrm{inj},t}, Q^{h,\omega}_{\mathrm{inj},t}\right)$ for $h \in \mathcal{H}$ is feasible. i.e., the voltages of the resultant load flow remain within limits described by:

$$\underline{v} \le |V_{i,t}| \le \overline{v}, \quad i \in \mathcal{N} \tag{16}$$

where $|V_{i,t}|$ is the magnitude of voltage in node i at time t, $\underline{v}$ and $\overline{v}$ are the lower and upper limits of voltages and $\mathcal{N}$ is the set of P-Q buses of the network.

Following this, the feasible region of operation in the P-Q plane for $h \in \mathcal{H}^{++}$ at time t, $\mathcal{B}^h_t \subseteq \mathfrak{B}^h_t \subset \mathbb{R}^2$, can be expressed as:

$$\mathcal{B}^h_t := \left\{ \left(P^{h,\omega}_{\mathrm{inj},t}, Q^{h,\omega}_{\mathrm{inj},t}\right), \omega \in \Omega \;\middle|\; \begin{array}{c} \text{satisfies (16)} \\ \text{load flow in [11]} \end{array} \right\} \tag{17}$$

Compared to a set of feasible pairs of $\left(P^h_{\mathrm{inj},t}, Q^h_{\mathrm{inj},t}\right)$ that would not violate voltage constraints at any node of the

[1] A household could utilise the existing home energy management system (HEMS) to perform this calculation.

network at a particular time step, the DNSP is interested in determining an envelope which represents the overall region of operation at the PoC for all $h \in \mathcal{H}^{++}$ at a certain time step. To this end, the *convex hull* [12] of $\left(P^h_{\text{inj},t}, Q^h_{\text{inj},t}\right)$ is constructed to determine the envelope of the PoC.

Let $x_\omega = \left[P^{h,\omega}_{\text{inj},t}, Q^{h,\omega}_{\text{inj},t}\right]^{\text{T}} \in \mathbb{R}^2$ be a feasible pair of power injection for house $h \in \mathcal{H}^{++}$ under scenario ω at time t, then the *convex hull* of all the feasible pairs of power injections for $h \in \mathcal{H}^{++}$ at time $t \in \mathcal{T}$, i.e., the *convex hull* of $\mathcal{B}^h_t$, can be obtained as:

$$\mathbf{conv}(\mathcal{B}^h_t) := \left\{ \sum_\omega \theta_\omega \, x_\omega \;\middle|\; \begin{array}{c} x_\omega \in \mathcal{B}^h_t \\ \theta_\omega \geq 0 \text{ for all } \omega \\ \sum_\omega \theta_\omega = 1 \end{array} \right\} \tag{18}$$

It is important highlighting that, considering the 2-D nature of the problem, the convex envelope defined in (18) reduces to a convex polygon as $\left(P^{h,\omega}_{\text{inj},t}, Q^{h,\omega}_{\text{inj},t}\right) \in \mathbb{R}^2$. Moreover, considering the *half-space representation* [12] for a convex polygon, $\mathbf{conv}(\mathcal{B}^h_t)$ can be expressed as:

$$\mathbf{conv}(\mathcal{B}^h_t) = \left\{ \left(P^h_{\text{inj},t}, Q^h_{\text{inj},t}\right) \middle| \mathbf{A} \cdot \left[P^h_{\text{inj},t}, Q^h_{\text{inj},t}\right]^{\text{T}} \leq \mathbf{b} \right\} \tag{19}$$

where $\mathbf{A} \in \mathbb{R}^{m \times 2}$ and $\mathbf{b} \in \mathbb{R}^m$ such that $m \leq |\mathcal{B}^h_t|$, $|\cdot|$ represents the cardinality of a set. To this end, the *convex hull* and parameters of its half-space representation can be calculated using existing software packages such as MATLAB, MPT-3 [13]. Once operating envelopes are calculated for a certain time step, the information is shared *DOE customers* for their demand response participation in market services.

Unlike explicit set-points determined based on a certain design objective as in OPF approaches [3], [5], the operating envelope obtained by constructing the *convex hull* outlines the region of operation in the P-Q plane—inclusive of active-reactive and import-export limits—without breaching voltage statutory limits.

B. Stage II: DRA controlling household air-conditioners to provide DR services

The objective of each *DOE customer* is to minimise the electricity cost based on a price signal. This includes maintaining the indoor temperature within thermal comfort limits and also managing the consumption at the PoC within the operating envelope sent by the DNSP.

Considering $h \in \mathcal{H}^{++}$ at time $t \in \mathcal{T}$, this can be expressed as an optimisation problem in the following form:

$$\min_{P^h_{\text{AC}}} \quad \pi^h_t \cdot P^h_{\text{con},t} \tag{20a}$$

subject to:

$$P^h_{\text{con},t} = P^h_{\text{AC},t} + \tilde{P}^h_{\text{UL},t} - \tilde{P}^h_{\text{PV},t} \tag{20b}$$

$$Q^h_{\text{con},t} = Q^h_{\text{AC},t} + \tilde{Q}^h_{\text{UL},t} - \tilde{Q}^h_{\text{PV},t} \tag{20c}$$

$$T^h_{\text{AC},t+1} = \exp\left(-\Delta t / R^h_{\text{AC}} \, C^h_{\text{AC}}\right) \cdot T^h_{\text{AC},t} + \left(1 - \exp\left(-\Delta t / R^h_{\text{AC}} \, C^h_{\text{AC}}\right)\right) \left(T^h_{\text{out},t} - \eta^h_{\text{AC}} \, R^h_{\text{AC}} \, P^h_{\text{AC},t}\right) \tag{20d}$$

$$\underline{T}^h_{\text{AC}} \leq T^h_{\text{AC},t} \leq \overline{T}^h_{\text{AC}} \tag{20e}$$

$$\mathbf{A} \cdot \begin{bmatrix} P^h_{\text{con},t} \\ Q^h_{\text{con},t} \end{bmatrix} \geq \mathbf{b} \tag{20f}$$

and (3)-(6)

where $P^h_{\text{con},t}$ and $Q^h_{\text{con},t}$ correspond to net active and reactive power consumption at the PoC, $T^h_{\text{AC},t}$ is the indoor temperature, $T^h_{\text{out},t}$ is the outdoor temperature and π^h_t is the electricity price for house h at time t. $\underline{T}^h_{\text{AC}}$ and $\overline{T}^h_{\text{AC}}$ represent lower and upper limits of thermal comfort, R^h_{AC} is the thermal resistance, C^h_{AC} is the thermal capacitance for the air-conditioning system and Δt is the sampling time [8]. Minimising the electricity cost is represented by (20a), active and reactive power balance at the PoC are represented by (20b) and (20c), thermal dynamics of the inverter-type air-conditioner is represented by (20d), thermal comfort limits are represented by (20e). (20f) is an alternative representation of the operating envelopes determined by (19). Since net consumption at the PoC is considered in (20) compared to net injections in (19), the sign of the inequality reverses.

The objective of the aggregator is to track the load set-point signal commanded by the market operator by controlling the consumption of air-conditioners belonging to *DOE customers*. This can be mathematically expressed as:

$$\min_{P^h_{\text{AC},t}} \quad \left(\sum_{h \in \mathcal{H}^{++}} P^h_{\text{AC},t} - P_{\text{ref},t} \right)^2 \tag{21}$$

where $P_{\text{ref},t}$ is the reference load set-point sent by the market operator at time t. According to (21), the deviation of the sum of air-conditioner power consumption from the load set-point is minimised.

Although the DRA could centrally control air-conditioning loads to track the load set-point signal [14], it will require *DOE customers* to share power ratings, R_{AC} and C_{AC} values, $\underline{T}_{\text{AC}}$ and $\overline{T}_{\text{AC}}$ limits for their own air-conditioners with the DRA. This will lead to end-user privacy violations. To overcome this, a hierarchical implementation based on the ADMM form of the *resource sharing problem* [15] is utilised. In this regard, a local controller at each *DOE customer* and a coordinating controller at the DRA are established.

1) Local controller problem

Considering household $h \in \mathcal{H}^{++}$, the local controller problem can be formulated as follows:

$$P_{\mathrm{AC},t}^{h(\nu+1)} = \underset{P_{\mathrm{AC},t}^{h}}{\operatorname{argmin}} \Bigg(\pi_t^h P_{\mathrm{con},t}^h + (\rho/2) \cdot \Big(P_{\mathrm{AC},t}^h - P_{\mathrm{AC},t}^{h(\nu)} + P_{\mathrm{avg},t}^{(\nu)} - P_t^{(\nu)} + \theta_t^{(\nu)} \Big)^2 \Bigg) \tag{22}$$

$$\text{subject to (3)-(6), (20b)-(20f)}$$

where (ν) represents ν-th iteration of the ADMM scheme, $\rho > 0$ is the augmented Lagrangian parameter, $P_{\mathrm{avg},t}$ is the average of $P_{\mathrm{AC},t}^h$, P_t is an auxiliary variable such that $P_t = (1/|\mathcal{H}^{++}|) \sum_{h \in \mathcal{H}^{++}} P_t^h$, and θ is the dual scaled variable. The interested readers are referred to [15] for more details on the scaled form of ADMM for the *sharing problem*.

2) Coordinating controller problem

For the coordinating controller at the DRA, the load set-point tracking problem in (21) is modified as:

$$P_t^{(\nu+1)} = \underset{P_t}{\operatorname{argmin}} \Bigg(\Big(|\mathcal{H}^{++}| P_t - P_{\mathrm{ref},t} \Big)^2 + \Big(|\mathcal{H}^{++}| \rho/2 \Big) \cdot \Big(P_t - \theta_t^{(\nu)} - P_{\mathrm{avg},t}^{(\nu+1)} \Big)^2 \Bigg) \tag{23a}$$

$$\theta_t^{(\nu+1)} = \theta_t^{(\nu)} + P_{\mathrm{avg},t}^{(\nu+1)} - P_t^{(\nu+1)} \tag{23b}$$

The tracking problem is represented by (23a) and the global dual variable update is represented by (23b).

To further explain this, in iteration ν at time step t, each local controller solves (22) to determine $P_{\mathrm{AC},t}^{h(\nu+1)}$ for all $h \in \mathcal{H}^{++}$ and passes to the coordinating controller. In the next step, the coordinating controller calculates the average of $P_{\mathrm{AC},t}^{h(\nu+1)}$ which is given by $P_{\mathrm{avg},t}^{(\nu+1)}$ and thereafter, solves (23a) to determine $P_t^{(\nu+1)}$. Finally, the coordinating controller updates the global dual variable as in (23b). This process is repeated at each iteration until the following termination criteria are met.

$$\|\mathbf{r}_t^{(\nu)}\|_2 \leq \epsilon^{\mathrm{prim}} \quad \text{and} \quad \|\mathbf{s}_t^{(\nu)}\|_2 \leq \epsilon^{\mathrm{dual}} \tag{24}$$

where $\mathbf{r}_t^{(\nu)}$ and $\mathbf{s}_t^{(\nu)}$ are the primal and dual residuals in ν-th iteration at time t, ϵ^{prim} and ϵ^{dual} are the tolerances for primal and dual residual respectively. Furthermore, $\mathbf{r}_t^{(\nu)} = [P_{\mathrm{AC},t}^{1(\nu)} - P_t^{(\nu)}, \ldots, P_{\mathrm{AC},t}^{n(\nu)} - P_t^{(\nu)}]$ for $\mathcal{H}^{++} := \{1, 2 \ldots, n\}$ and $\mathbf{s}_t^{(\nu)} = [P_t^{(\nu+1)} - P_t^{(\nu)}]$. In addition to the termination criteria given by (24), criteria based on maximum ADMM iteration to terminate, *maxiter*, can be imposed to speed up the ADMM algorithm.

III. Results

To validate the proposed approach, it is assumed that the DRA receives a load set-point signal that should be tracked for a period of 2-hours, starting at 10:00 and ending at 12:00, on 06/12/2020. The validations are performed on a practical residential network in Queensland, Australia [16]. The single-line diagram of the residential network is given shown in Fig. 2. Since network data is only available up to the pole level, it is considered that nodes represented by (2)-(35) has a single customer connected to each of the three phases. This results in a total of $34 \times 3 = 102$ customers. Aligned with statistical data from [17], it is assumed that $\approx 45\%$ (46 out of 102) households are equipped with rooftop PV generation. The ratings of the PV inverter are [3.0, 3.6, 4.0, 5.0, 6.0, 8.0] kWp [18] with $\varphi_{\mathrm{PV}}^h = 0.8$ for all $h \in \mathcal{H}^{++} \cup \mathcal{H}^{+}$ in line with [1], [10]. For uncontrollable loads, $\varphi_{\mathrm{UL}}^h = 0.95$ (lagging) [1]. For inverter-type air conditioners, $\varphi_{\mathrm{AC}}^h = 0.95$ based on the power factor correction method [9], $\overline{P}_{\mathrm{AC}}^h \sim \mathcal{N}(2.5, 3.5)$ kW; $R_{\mathrm{AC}}^h \sim \mathcal{N}(1.5, 2.5)$ °C/kW; $C_{\mathrm{AC}}^h \sim \mathcal{N}(1.5, 2.5)$ °kWh/°C; $\eta_{\mathrm{AC}}^h = 2.5$, $\underline{T}_{\mathrm{AC}}^h = 22$°C and $\overline{T}_{\mathrm{AC}}^h = 24$°C and the initial temperature $T_{\mathrm{AC},t=0}^h$ is considered to be 23°C for all $h \in \mathcal{H}^{++}$. The outdoor temperature profile is obtained from [19]. The load set-point signal is constructed as in [14] considering the set-point temperature to be 23°C and a regulation capacity of 20% from the baseline consumption. The profiles for household uncontrollable load and rooftop PV generation are obtained from [20]. The household electricity prices are obtained from the National Electricity Market (NEM) [21].

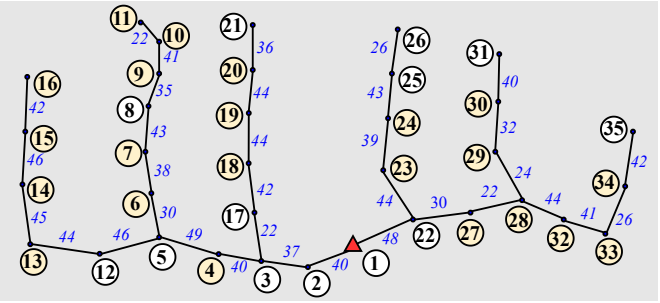

Fig. 2. The single line diagram of the LV residential network [16]; bus (1) (red triangle) represents the LV distribution transformer; black dots (bus (2) – bus (35)) represent P-Q buses (poles); a household is connected to each phase of each bus except (1); black lines represent overhead conductors; italicised numbers in blue represent pole-to-pole and transformer-to-pole distances in metres; poles with *DOE customers* are highlighted in yellow

The three-phase network is modelled in OpenDSS [22] with voltage statutory $\underline{v} = 0.95$ pu and $\overline{v} = 1.10$ pu [1]. The overall algorithm is written in MATLAB on a desktop computer equipped with an Intel(R) Core i7 3.20 GHz CPU and 16 GB RAM memory. The optimisation problems discussed in section II are modelled with YALMIP toolbox [23] and solved with Gurobi 9.1.2 [24]. The *convex hull* and its half-space representation are calculated using MPT-3 [13]. For the ADMM problem, ϵ^{prim} and ϵ^{dual} are `1e-3`, ρ =1 and *maxiter* = 15. The simulation step size Δt =5-min, i.e., DOEs are assigned every 5-mins, aligned with the market clearing interval of the NEM [2].

Considering a total of 30 *DOE customers* ($\approx$ 30%) and 500 MC load flow scenarios, i.e., $|\Omega| = 500$, simulation studies are carried out to determine the overall performance of the proposed control scheme. The process involved in determining the bounding box based on power injection limits and thereafter estimating the operating envelope based on *convex hull* method for house 38 connected to bus (14) at 11:15 is given in Fig. 3.

It can be seen from Fig. 4a that the DRA is able to follow the load set-point signal with a high accuracy, error < 0.004 kW, for the DR period considered. Looking at Fig. 4b it is observed that the indoor temperature for *DOE customers* remain within thermal comfort limits $[22, 24]$°C throughout the DR period. Hence, it can be concluded that, under the proposed hierarchical control scheme, the thermal comfort of *DOE customers* is not compromised even though the DRA accurately follows the load set-point signal by controlling the consumption of air-conditioners owned by *DOE customers*.

Discussing the scalability of the proposed approach, the average execution time per step is around 50 seconds which is far less than 5-mins—the sampling interval (Δt). Hence, it can be claimed that the overall approach is scalable.

IV. Conclusions

In this work, a two-stage approach is proposed for residential DR to provide market services under the dynamic operating envelopes framework. In the first stage, the DNSP employs a *convex hull* method to determine household operating envelopes. In the next step, the DRA controls household air-conditioning loads to follow a load set-point signal in the electricity market. The simulation results suggest that the load set-point signal can be tracked with an error margin in the order of 10^{-3} kW while maintaining the indoor temperature within $[22, 24]$°C limits. Furthermore, the approach is scalable.

Acknowledgment

The author would like to thank for the support given by the Centre for Energy Data Innovation (CEDI), The University of Queensland, under the Advance Queensland grant (grant no: AQPTP01216-17RD1).

References

[1] ENERGEX Limited, "STNW3510: Dynamic Standard for Small IES Connections." https://www.ergon.com.au/__data/assets/pdf_file/0004/962779/STNW3510-Dynamic-Standard-for-Small-IES-Connections.pdf.

[2] Dynamic Operating Envelopes Working Group, "Outcomes Report." https://arena.gov.au/assets/2022/03/dynamic-operating-envelope-working-group-outcomes-report.pdf.

[3] M. Z. Liu, L. F. Ochoa, and S. Member, "Using OPF - Based Operating Envelopes to Facilitate Residential DER Services," *IEEE Transactions on Smart Grid*, no. June, p. 1, 2022.

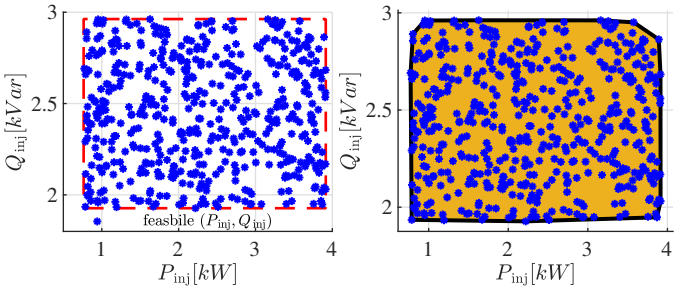

(a) Bounding box (capability curve) (b) Convex hull

Fig. 3. The bounding box representing the capability curve and the convex hull representing the envelope at the PoC for house 38 connected to bus (14) at 11:15. $|\Omega| = 500$

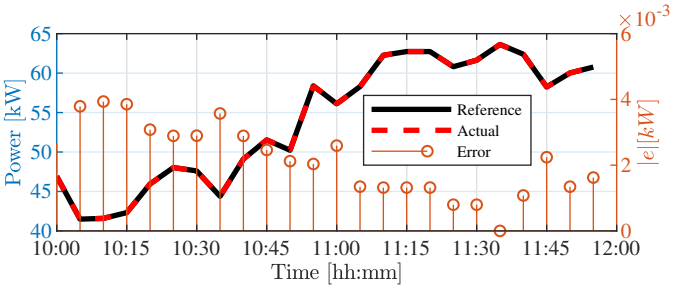

(a) Tracking performance of the DRA

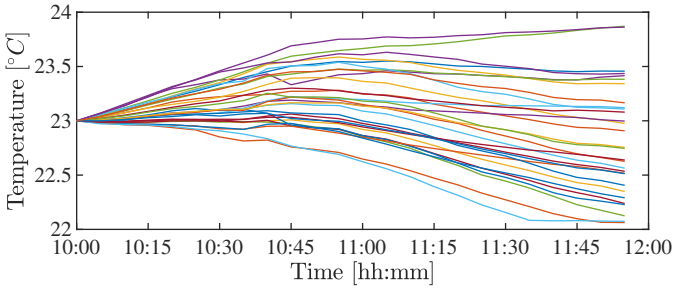

(b) The variation of indoor temperature for *DOE customers*

Fig. 4. The bounding box representing the capability curve and the convex hull representing the envelope at the PoC for house 38 connected to bus (14) at 11:15. $|\Omega| = 500$

[4] K. Petrou, A. T. Procopiou, L. Gutierrez-Lagos, M. Z. Liu, L. F. Ochoa, T. Langstaff, and J. M. Theunissen, "Ensuring distribution network integrity using dynamic operating limits for prosumers," *IEEE Transactions on Smart Grid*, vol. 12, pp. 3877–3888, Sep. 2021.

[5] A. Attarha, S. M. N. R.A., P. Scott, and S. Thiebaux, "Network-Secure Envelopes Enabling Reliable DER Bidding in Energy and Reserve Markets," *IEEE Transactions on Smart Grid*, p. 1, 2021.

[6] V. Rigoni, D. Flynn, and A. Keane, "Coordinating Demand Response Aggregation with LV Network Operational Constraints," *IEEE Transactions on Power Systems*, vol. 36, pp. 979–990, mar 2021.

[7] R. Gupta, F. Sossan, and M. Paolone, "Grid-Aware Distributed Model Predictive Control of Heterogeneous Resources in a Distribution Network: Theory and Experimental Validation," *IEEE Transactions on Energy Conversion*, vol. 36, pp. 1392–1402, jun 2021.

[8] J. L. Mathieu, S. Koch, and D. S. Callaway, "State Estimation and Control of Electric Loads to Manage Real-Time Energy Imbalance," *IEEE Transactions on Power Systems*, vol. 28, pp. 430–440, feb 2013.

[9] Lazar Rozenblat, "The basics of active power factor correction." https://www.powerfactor.us/active.html.

[10] Standards Australia, "Grid connection of energy systems via inverters, Part 2: Inverter requirements." https://www.standards.org.au/standards-catalogue/sa-snz/other/el-042/as-slash-nzs--4777-dot-2-colon-2020.

[11] V. Rigoni and A. Keane, "Open-DSOPF: an open-source optimal power flow formulation integrated with OpenDSS," in *2020 IEEE Power & Energy Society General Meeting (PESGM)*, pp. 1–5, aug 2020.

[12] M. T. De Berg, M. Van Kreveld, M. Overmars, and O. Schwarzkopf, *Computational geometry: algorithms and applications*. Springer Science & Business Media, 2000.

[13] M. Herceg, M. Kvasnica, C. Jones, and M. Morari, "Multi-Parametric Toolbox 3.0," in *Proc. of the European Control Conference*, (Zürich, Switzerland), pp. 502–510, July 17–19 2013. http://control.ee.ethz.ch/~mpt.

[14] N. Lu, "An evaluation of the HVAC load potential for providing load balancing service," *IEEE Transactions on Smart Grid*, vol. 3, no. 3, pp. 1263–1270, 2012.

[15] S. Boyd, N. Parikh, E. Chu, B. Peleato, and J. Eckstein, "Distributed Optimization and Statistical Learning via the Alternating Direction Method of Multipliers," *Found. Trends Mach. Learn.*, vol. 3, pp. 1–122, jan 2011.

[16] L. Wang, R. Yan, and T. K. Saha, "Voltage regulation challenges with unbalanced PV integration in low voltage distribution systems and the corresponding solution," *Applied Energy*, vol. 256, p. 113927, 2019.

[17] Australian PV Institute, "Mapping Australian Photovoltaic Installations." https://pv-map.apvi.org.au/historical.
[18] SMA Solar Technology AG, "SUNNY BOY 3.0/3.6/4.0/5.0." https://www.sma.de/fileadmin/content/global/specials/documents/falcon-installer/SB30-50-DEN1708-V22web.pdf.
[19] School of Earth and Environmental Sciences, The University of Queensland, "UQ weatherstations." http://ww2.sees.uq.edu.au/uqweather/.
[20] E. McKenna and M. Thomson, "High-resolution stochastic integrated thermal–electrical domestic demand model," *Applied Energy*, vol. 165, pp. 445–461, 2016.
[21] Australian Energy Market Operator, "NEM data dashboard." https://aemo.com.au/en/energy-systems/electricity/national-electricity-market-nem/data-nem/data-dashboard-nem.
[22] R. C. Dugan and T. E. McDermott, "An open source platform for collaborating on smart grid research," in *2011 IEEE Power and Energy Society General Meeting*, pp. 1–7, 2011.
[23] J. Löfberg, "YALMIP: A toolbox for modeling and optimization in MATLAB," in *Proceedings of the IEEE International Symposium on Computer-Aided Control System Design*, (Taipei, Taiwan), pp. 284–289, 2004.
[24] L. L. C. Gurobi Optimization, "Gurobi Optimizer Reference Manual." http://www.gurobi.com, 2021.